Journal Pre-proofs

S. Stekovic, J.P. Jones, B. Engel, M.T. Whittaker, V. Norman, J.P. Rouse, S. Pattison, C.J. Hyde, P. Härnman, R.J. Lancaster, D. Leidermark, J. Moverare

Please cite this article as: Stekovic, S., Jones, J.P., Engel, B., Whittaker, M.T., Norman, V., Rouse, J.P., Pattison, S., Hyde, C.J., Härnman, P., Lancaster, R.J., Leidermark, D., Moverare, J., DevTMF – Towards Code of Practice for Thermo-Mechanical Fatigue Crack Growth, *International Journal of Fatigue* (2020), doi: https://doi.org/10.1016/j.ijfatigue.2020.105675

This is a PDF file of an article that has undergone enhancements after acceptance, such as the addition of a cover page and metadata, and formatting for readability, but it is not yet the definitive version of record. This version will undergo additional copyediting, typesetting and review before it is published in its final form, but we are providing this version to give early visibility of the article. Please note that, during the production process, errors may be discovered which could affect the content, and all legal disclaimers that apply to the journal pertain.

DevTMF – Towards Code of Practice for Thermo-Mechanical Fatigue Crack Growth

S. Stekovic[a], J. P. Jones[b], B. Engel[c], M. T. Whittaker[b], V. Norman[a], J. P. Rouse[c], S. Pattison[d], C. J. Hyde[c], P. Härnman[a], R. J. Lancaster[b], D. Leidermark[e] and J. Moverare[a]

[a]Division of Engineering Materials, Department of Management and Engineering, Linköping University, SE-581 83 Linköping, Sweden
[b]Institute of Structural Materials, Swansea University, SA1 8EN Swansea, UK
[c]Gas Turbine and Transmission Research Centre, G2TRC, Faculty of Engineering, University of Nottingham, NG7 2TU, Nottingham, UK
[d]Rolls-Royce plc, DE24 8BJ, Derby, UK
[e]Division of Solid Mechanics, Department of Management and Engineering, Linköping University, SE-581 83 Linköping, Sweden

Abstract

The current paper presents work on identification and evaluation of a range of factors influencing accuracy and comparability of data generated by three laboratories carrying out stress-controlled thermo-mechanical fatigue crack growth tests. It addresses crack length measurements, heating methods and temperature measurement techniques. It also provides guidance for pre-cracking and use of different specimen geometries as well as Digital Image Correlation imaging for crack monitoring. The majority of the tests have been carried out on a coarse grain polycrystalline nickel-base superalloy using two phase angles, Out-of-Phase and In-Phase cycles with a triangular waveform and a temperature range of 400-750 $^{\circ}$C.

Keywords: code of practice, crack growth, experiment development, internal round robin, thermo-mechanical fatigue

1. Introduction

DevTMF is a research project funded by the EU Framework Programme for Research and Innovation Horizon 2020 and Clean Sky 2, with an aim to characterise thermo-mechanical fatigue (TMF) behaviour of structural alloys of interest to allow for more accurate prediction of design lives of present and future gas turbine components. DevTMF stands for Development of Experimental Techniques and Predictive Tools to Characterise Thermo-Mechanical Behaviour and Damage Mechanisms and is focused on contributing to development of new materials and improving efficiency of aero engine components that will reduce fuel consumption and environmental impact. This is ultimately achieved by either introduction of novel engine design or development of new materials able to sustain complex loadings from take-off, cruise, descent and shut down. Specifically, TMF, which occurs at the rim of turbine discs, aero-foils and rear structures, requires assessment in terms of both crack initiation and crack propagation as the harsh thermal transients during take-off and descent may cause the formation of cracks. Apart from work on strain-controlled TMF, DevTMF has been aiming to evaluate and develop TMF crack growth (CG) methods that are essential to demonstrate structural integrity and certification requirements of being tolerant of handling damage as well as to assess remaining lives in cracked turbine components.

A previous European project on TMF funded by the EU FP5 [1], which ended in 2005, was successful at evaluating and addressing issues related to strain controlled TMF testing. This project led to the development of a well-known Code of Practice (CoP) for strain controlled TMF test [2], which has been implemented by testing facilities and equipment manufacturers worldwide. Together with ASTM E2368 Standard Practice for Strain Controlled Thermomechanical Fatigue Testing [3] and ISO 12111:2011 Standard for Strain-controlled thermomechanical fatigue testing method [4], the CoP provides thorough recommendations and guidance for setting up, performing and analysing strain-controlled TMF tests. However, TMF CG is still an emerging field, and unlike strain controlled TMF, is not yet covered by a code of practice and/or an international standard. Hence, the initial focus of the work in this project has been based on interlaboratory harmonisation of the TMF CG test method between the partners through a project internal TMF CG round robin exercise, in particular with respect to appropriate heating and cooling methods, crack monitoring techniques and specimen design. All tests were performed at the same temperature range of 400-750 ºC. The main aim of the internal round robin has been to establish a local code of practice for the tests ensuring repeatability and consistency to generate high-quality accurate data for life prediction modelling.

The three participating laboratories that were involved in this round robin testing are (1) Division of Engineering Materials, Linköping University, Linköping, Sweden, (2) Institute of Structural Materials/Sefydliad Deunyddiau Strwythurol, Swansea University, Swansea, UK, and (3) Gas Turbine and Transmission Research Centre, G2TRC, Faculty of Engineering, the University of Nottingham, Nottingham, UK.

2. Experimental procedures

2.1. Material

The participating laboratories have used the coarse grain nickel-base superalloy RR1000 for the internal TMF CG round robin testing. The material is processed by a powder metallurgy route and strengthened by Ni_3Al-type γ' precipitates. The nominal chemical composition in wt. % and details about the processing as well as the heat treatment of the alloy are given in [5]. The microstructure typically consists of grain sizes of ASTM 7-3 (32-125μm). Apart from the γ matrix and main strengthening secondary and tertiary γ' phases, the material also contains a dispersed sub-micron phases such as MC carbides and M_3B_2 borides. Both γ' precipitates are intergranular distributed with the γ' varying in size from 1 μm to 5 nm depending on the heat treatment and cooling rates [6] [7].

2.2. Specimen geometries

Since the testing and measurement equipment between the laboratories vary, two different types of test specimens have been adapted for the round robin. The specimens were taken out of forgings and randomly selected to be machined as either one of the two specimen designs.

At Swansea University, a 7 mm square corner crack specimen design was used, Figure 1b. A sharp notch approximately 0.35 mm deep, was machined into one of the four corners in the middle of the gauge section by using a diamond edge sawblade. The geometry ensured that cracks with a quarter-circular shape were produced.

2

At Linköping University and the University of Nottingham, a single edge notch (SEN) type specimen with circular cross-section at the ends and a rectangular cross-section in the gauge was used, Figure 1a. The ends of the specimens were slightly different between the laboratories as the ends were adopted to gripping system used. Note that the gauge (middle) section was the same for all specimens, having an approximately rectangular cross-section with a thickness of 3 mm and a width of 12 mm. A sharp 3 mm deep notch with a radius of 1 mm was machined with electrical discharge machining (EDM) at the centre of the gauge length, which was used to initiate a starting crack.
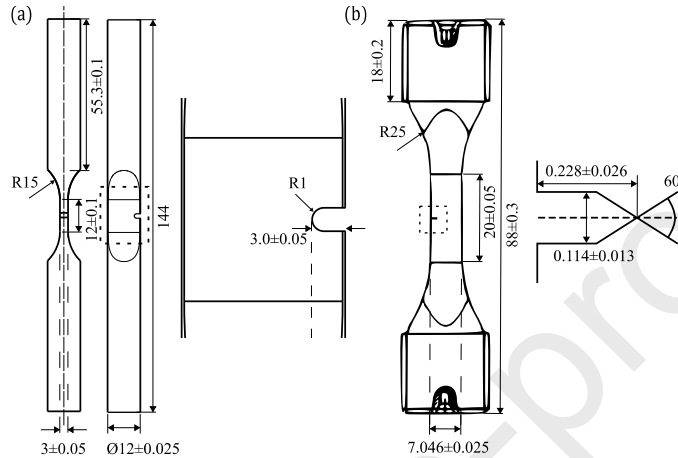

Figure 1: (a) Single edge notched and (b) corner crack specimen geometry used for the internal TMF crack growth round robin tests

All SEN test pieces were machined by turning and wire EDM without any surface improvement treatment afterwards. Corner crack specimens were machined at P S Marsden (Precision Engineering) Ltd in the UK, while the SEN specimens were machined at Linköping University.

2.3. Equipment and heating methods

The project internal TMF CG round robin tests were undertaken on two bespoke test setups at Swansea University. The first setup included an Instron 100 kN servo-hydraulic test frame with a Zwick CUBAS control system and a Trueheat 10 kW induction coil heating with forced air cooling using four Meech pneumatic air amplifiers. However, before starting the testing, different coil designs as well as effect of crack tip heating were investigated since eddy currents generated by induction coil heating might interact with the direct current potential drop (DCPD) currents creating noise and interference [8]. Therefore, various coil designs and cooling methods were investigated to provide the most appropriate balance between axial and radial thermal gradients, desired heating and cooling rates as well as best line of sight towards the fatigue crack starter notch, enabling investigations of preferential crack tip heating. Investigations of the coil designs by using non-invasive infra-red thermography cameras did not show any excessive heating of the crack tip in the investigated nickel-base alloy due to relatively high thermal conductivity associated with nickel [9]. The second setup comprised of an Instron 100 kN servo-electric test frame with a DARTEC control system and a second-generation 12 kW radiant lamp furnace (RLF) designed in collaboration with Severn Thermal Solutions Ltd as a split body design with each half containing three horizontally mounted lamps. Thus, the tests were undertaken on both infrared and induction heating setups. No influence of heating method was found using nickel specimens, Figure 2.
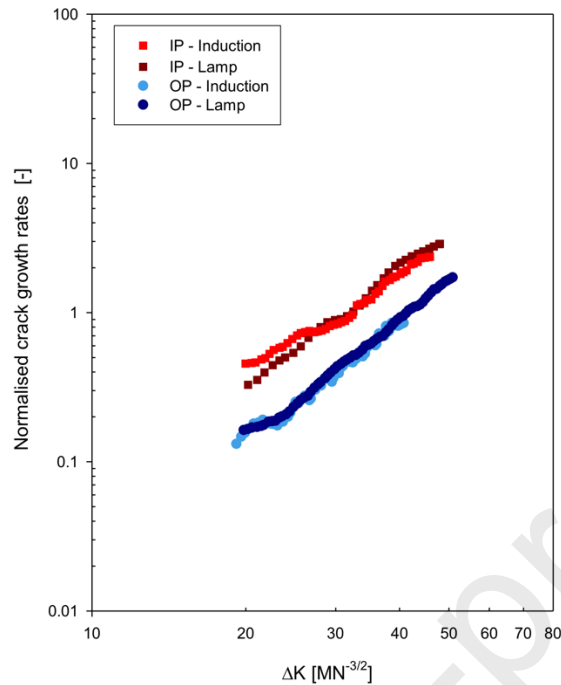
Figure 2: Comparison between TMF in-phase (IP) and out-of-phase (OP) crack growth rates measured using induction and lamp furnace heating.

At Linköping university, the TMF crack growth testing was conducted in air using a servo-hydraulic Instron 8802 test machine equipped with a 100 kN load cell and a Hüttinger induction heating system, model TIG3/500, with a circular copper coil and compressed air flow directed towards the specimen through three circumferentially positioned nozzles for cooling. All tests were controlled and monitored using a dedicated TMF software developed by Instron, which automatically performs a pre-test procedure, involving thermal stabilisation, thermal strain measurement and validation. In addition, an elastic modulus measurement programme, included in the software, was run prior each test, measuring the elastic modulus at different temperatures using load cycles of ±20 MPa. An axial 12.5 mm gauge length Instron high-temperature extensometer, model 2632-055, was mounted over the notch on the specimens in the gauge section. The temperature was measured using a N-type thermocouple spot-welded in the centre of the side surface of the specimen, slightly beneath the expected crack path.

At the University of Nottingham, the tests were performed on an Instron 8862 servo electric 35 kN TMF system, which utilizes a water cooled variable frequency, induction generator rated at 10kW, in order to allow for rapid heating of the test specimen. In addition, external forced air cooling was used to increase the achievable rate of cooling.

2.4. Temperature measurements

Invasive and non-invasive temperature control systems comprising N-type thermocouples, pyrometry and infra-red thermography with HE23 paint were investigated at Swansea University [9], before starting of the project internal TMF CG round robin exercise. Thermocouples were used to obtain a baseline temperature and also because they have been the widely accepted measurement

4

method in most mechanical testing. The thermocouples were spot-welded to measure temperature at the test-piece surface from the upper, lower and centre locations of the gauge section. These temperatures were then used to validate measurements taken from thermography, Micro-Epsilon TIM640 and TIM M1, and pyrometry, CT 3MH2 CF and CT XL 3MH3 CF3, at the same locations on the test specimen. Prior to any testing, rigorous thermal profiling was undertaken using six, 0.2mm Ø N-type thermocouples. Thermocouples were spot-welded at the centre gauge location on each of the four rectangular specimen faces to realise the radial heating gradient. A further two thermocouples were spot-welded 5mm above and below a centre thermocouple to generate axial temperature distributions. As no TMF CG standard currently exists, the stringent temperature limits were imposed by the governing TMF strain control standards, [3] [4]. A typical temperature distribution with a spread of ±3°C was achieved around the crack.

Before the start of the test series at Linköping University, thermal profiling between 400-750°C was conducted in order to evaluate the temperature distribution on the specimen. For this purpose, six different N-type thermocouples were attached by spot-welding to a dummy specimen at different locations; three on each side evenly distributed along the axial centre line of the specimen. By monitoring the temperature at each thermocouple, the coil and air nozzles were adjusted in order to achieve a temperature difference less than ±10 °C throughout the selected temperature cycle, as recommended by [3] and [4].

Spot-welded K-type thermocouples, with a wire diameter of 0.25 mm, were used for all temperature measurements at the University of Nottingham. For thermal calibration of the induction coil (i.e. in order to ensure temperature uniformity in the gauge section of the test sample), thermocouples were spot-welded as shown in Figure 3, in order to provide both axial and "radial" temperature uniformity in the specimen gauge length.
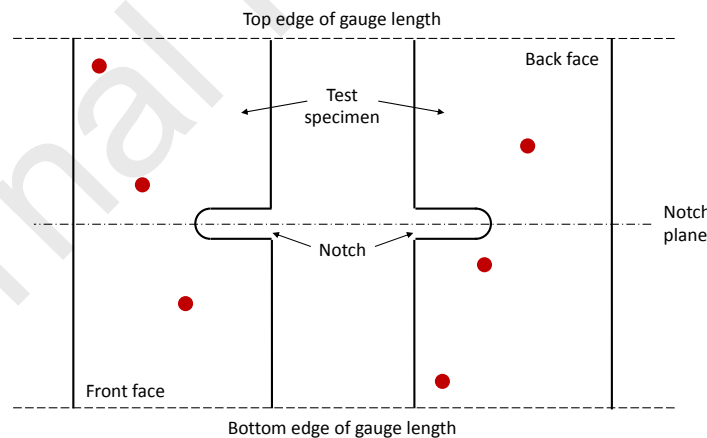

Figure 3: Schematic representation of the positions of the K-type thermocouples used for pre-test thermal calibration of the test machine at the University of Nottingham

Static and dynamic temperature gradient testing was carried out across the temperature range of 400 °C to 750°C to ensure the total temperature range within the gauge section was less than ±5 °C. For the performance of TMF testing, a control thermocouple was spot-welded as shown in Figure 4 with a target spacing of 1mm below and to the side of the notch tip (in order to avoid interaction between the crack and the spot-weld). A second thermocouple was welded in one of the gauge length corners, on the opposite face to the control thermocouple (also

5

shown in Figure 4), thereby acting as a guard and providing control in case of the loss of the main control thermocouple.
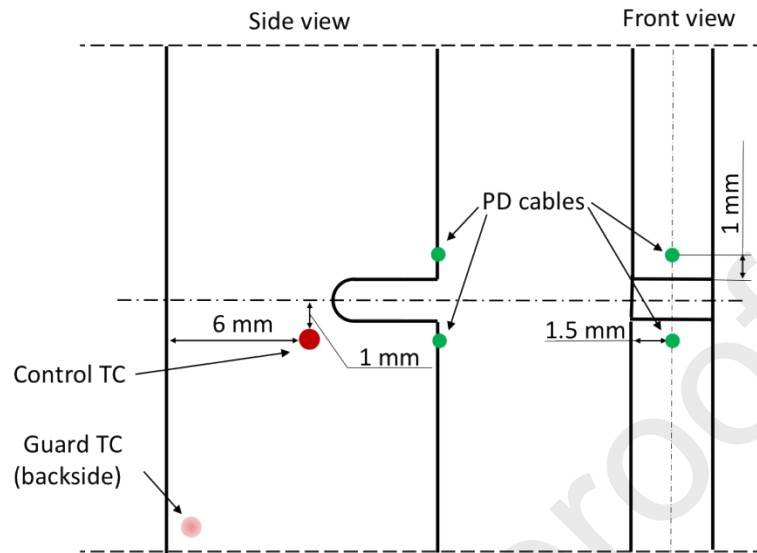

Figure 4: Schematic representation of the positions of the K-type thermocouples (TC) used for the testing at the University of Nottingham

2.5. Crack length measurements

In order to measure crack growth rates, three different crack length measurements methods were utilised in the project and described below. Data reported followed recommendations from the ASTM E647 standard, [10].

2.5.1.   Direct current potential drop

DCPD difference technique was utilised to monitor crack growth at Swansea University. A constant current was applied through the specimen, and the potential difference (PD) across the mouth of the crack was measured. As the crack grows, the resistance of the specimen increases, leading to an increase in PD. The change of PD is recorded as a function of time, and then converted to the crack length based on as appropriate PD-crack length calibration curve for a specific specimen geometry. A Dirlik control system was used to record crack length against number of cycles (a vs N) readings through pulsing a 10 A signal and utilising DCPD. This is then converted into da/dN data by using the incremental polynomial method, as described in the ASTM 647 appendixes [10]. The grips of the specimen were electrically insulated to avoid short circuiting of the DCPD system.

2.5.2.   Compliance method

The crack length as a function of number of cycles was determined at Linköping University by using the compliance method in accordance with a previous investigation involving the same specimen geometry [11] [12] and the guidelines from ASTM E647-08 [10]. The method uses the fact that the stiffness of the tested specimen changes as the crack grows, i.e. stiffness of the specimen decreases with increasing crack length. To this end, a finite element model of the

6

specimen was established based on its nominal dimensions given in Figure 1a. For this geometry, a linear-elastic material model and boundary conditions corresponding to isothermal and uniaxial tension were assigned in order to acquire the normalised specimen stiffness, which is defined as the slope of the modelled stress-strain curve at a given crack length divided by the slope observed when the crack length is zero. Note that the stress and the strain used to compute the slope were defined in the same way as in the experiments. In this way, an estimate of the normalised stiffness as a function of crack length was obtained by running the model with an added planar crack emanating from the notch by varying the crack length, see for instance [12]. Using this calibration curve, the experimental crack length was estimated based on the measurement of the normalised specimen stiffness in the crack growth tests. More precisely, the experimental stiffness was measured during the unloading segment starting at the instant of maximum load in each hysteresis loop.

2.5.3. Alternating current potential drop

Crack length measurements during testing at the University of Nottingham were carried out using the alternating current potential drop (ACPD) method. A MATELECT CGM-7 device was used as an AC generator with an applied frequency of 107 Hz (note that, for nickel-base materials, this is sufficiently low to result in a pseudo-DC response). In order to avoid interference between the induction heating system (also an AC system) and this ACPD system, an ACPR-2 pre-amplifier was used to cut-off the high frequency interference. Spot-welding was used to attach the ACPD measurement wires to the test specimen. The position of the wires can be seen in Figure 4.

2.6. Test conditions

All IP and OP TMF crack growth tests were carried out in laboratory air under stress control at different stress levels depending on the specimen geometry with a load ratio of R = 0 in triangular waveform. All tests were initiated under tension load. Total cycle time was 70 s with the temperature varying between 400 °C and 750 °C. In total, 9 specimens were tested under IP and 4 under OP test conditions. Heating and cooling rates were at 10 °C/s.

The test end condition was defined as a potential drop of change of 1.5 V, corresponding to crack length of approximately 4.5 mm at Swansea University. At Linköping University, all tests were stopped at a crack length of 4.2 mm. The tests at the University of Nottingham were stopped when a PD change of 1.5 V was measured during the test, because of a crack length close to critical values. After reaching the PD limit, the specimen was fatigued in stress control to final failure at room temperature and at 1 Hz. Post fractography analysis of the tests revealed that a PD change of 1.5 V is equal to a total crack length of around 4.5 mm.

2.7. Pre-cracking procedure

Swansea University developed a three-stage load shedding pre-cracking procedure conducted at room temperature in the project to avoid multiple crack initiation sites, [8]. The first stage was conducted at 120% of the test load with a frequency of 5 Hz, which was reduced to 100% of the test load in the 2nd stage. Then, the frequency was reduced to 1 Hz in the final stage keeping the same load as in the 2nd stage. Cycles to detect crack propagation was based on number of cycles required

7

to produce a detectible increase in the DCPD signal that was 25 µV in the 1st stage, 50 µV in the 2nd stage and 75 µV in the last stage. This procedure has resulted in TMF CG testing being reliable and repeatable.

At Linköping University, a different pre-cracking procedure was conducted to initiate and propagate a starting crack to a reasonable length in the test machine. The pre-cracking procedure was varied for the first two specimens until an optimised procedure regarding minimal duration and applied stress was established. For this reason, the procedure was not the same for the remaining three specimens. Load ratio for the first two specimens was R = 0 and then changed to R = -1 to accelerate pre-cracking procedure. Subsequent propagation to reach a reasonable starting crack length was done in a stepwise manner reducing the maximum stress with steps of 30 MPa in order to propagate through any eventual plastic zone caused by the previous maximum stress value. The maximum stress for pre-cracking varied between 300 and 210 MPa. At the end of the pre-cracking procedure for each specimen, the crack had a length of about 1 mm. It should also be noted that one of the tests (LiU-1) was initiated and propagated using the same temperature cycle as the actual test with the purpose of investigating the effect of a TMF initiated starting crack. Otherwise, the pre-cracking was done at room temperature.

At the University of Nottingham, specimen pre-cracking was performed at room temperature using an Instron 1341 servo-hydraulic machine under stress control at a frequency of 20 Hz and a load ratio of R = 0.1. ACPD signals were used to monitor crack initiation and propagation using the system described previously in section 2.5.3. In addition, an optical travelling microscope was attached to the test frame and used as a secondary crack length determination. The difficulty in using this optical system as a sole crack length measurement is that any tunneling of the crack cannot be observed. For crack initiation, a maximum stress amplitude of σ_{max} = 240 MPa was applied to the specimen until the ACPD measurement indicated a crack initiation by showing a derivation from the un-cracked specimen and the crack was confirmed using an optical microscope (under tension in order to exploit crack opening). After initiation, the maximum stress amplitude was reduced to σ_{max} = 210 MPa in order to slow down the crack propagation to a controllable rate. The crack length was measured via light microscope every 5000 cycles until a total pre-crack length of 1 mm was measured optically.

2.8.   K and ΔK evaluations

Stress intensity factor has been calculated for each load cycle using the well-known Eq. 1 where σ is applied stress, a is crack length, W is width of specimen and Y(a/W) is geometry factor.

$$K = Y\left(\frac{a}{W}\right) \times \sigma \times \sqrt{\pi \times a} \qquad (1)$$

At Swansea University, PD crack length calibration curves were used to relate the measured PD to the crack length for a corner crack specimen. The ΔK calculation at each point in the test is as shown in Eq. 2 and Eq. 3 where ΔK_n is the stress intensity factor range, a_n is the crack length at sample n and P is the load.

$$\Delta K_n = \frac{y_n \times \Delta P_n \times \sqrt{\pi \times a_n}}{Width \times Thickness} \qquad (2)$$

8

$$\Delta P_n = P_{max} - P_{min} \qquad (3)$$

The propagation compliance function y_n consists of four components expressed in Eq. 4.

$$y_n = M_G \times M_B \times M_S \times \frac{2}{\pi} \qquad (4)$$

where M_G, M_B and M_S are correction factors and generally functions of a_n/W with W as the specimen width, [13]. Their values are calculated as follows:

$$If\ 0 \le \frac{a_n}{W} \le 0.2\ then$$

$$M_G = 1.143$$

$$M_B = 1 + 0.06\left(\frac{a_n}{W}\right)$$

$$M_S = 1 + 0.07\left(\frac{a_n}{W}\right)$$

If $0 \le a_n/W \le 0.2$ then

$M_G = 1.143$
$M_B = 1 + 0.06*(a_n/W)$
$M_S = 1 + 0.07*(a_n/W)$

If $0.2 < a_n/W \le 0.2$ then

$M_G = 0.1*(a_n/W)^2 + 0.29*(a_n/W) + 1.081$
$M_B = 0.75*(a_n/W)^2 - 0.185*(a_n/W) + 1.019$
$M_S = 0.9*(a_n/W)^2 - 0.21*(a_n/W) + 1.02$

The compliance function presented here only applies to surface cracks. The function calculated at the 45° position is achieved by multiplying the compliance at the 90° position by the ratio of the results at the 45° and 90° positions as shown in Eq. 5.

$$y_n = y_n \times \left[0.9335 - 0.0045\frac{a_n}{W} + 0.1295\left(\frac{a_n}{W}\right)^2 - 0.4845\left(\frac{a_n}{W}\right)^3\right] \qquad (5)$$

At Linköping University, the stress-intensity factor was estimated from the same FE model as in the compliance method used for assessing the crack length, see section 2.5.2. Rearranging the general expression of the stress-intensity factor, the geometrical parameter Y as a function of crack length was obtained from computing the stress-intensity factor $\tilde{K}_I$ at a prescribed nominal stress $\tilde{\sigma}_{Max}$ and crack length a, i.e. Eq 6.

$$Y(a) = \frac{\tilde{K}_I}{\tilde{\sigma}_{Max}\sqrt{\pi a}} \qquad (6)$$

Again, the model was run with a linear-elastic material model and boundary conditions representing isothermal uniaxial loading. Thus, using this estimate of the geometrical parameter Y, the stress-intensity factor of a given experimental cycle was assessed based on the recorded nominal stress of the experiment and the crack length estimated by the compliance method.

A linear function was used to describe the crack length vs. potential drop measurement, using 2 points at the University of Nottingham. These points were the pre-test (pre-crack) crack length and the final crack length from the post-test fracture surface, determined by optical microscope, along with the corresponding PD measurements. This linear function was then used to determine the crack length for each cycle. Stress intensity factor was then calculated by using Eq. 1 while Y was evaluated by FE calculations according to the results from Linköping University.

3.   Results and discussion

3.1 OP TMF crack growth round robin results

Figure 5 shows TMF crack growth curves for the OP test conditions as a function of the stress intensity factor range for the investigated coarse grained material. It is seen that there is no difference in the response between the specimen types and the methods applied. This means that dependence of pre-cracking procedure, applied loads, microstructure and specimen type was minimal. As the stress intensity range is calculated from the applied load and the geometry of the specimen according to Eq. 1, the difference in ΔK from Figure 5 corresponds to variation in the applied stresses.
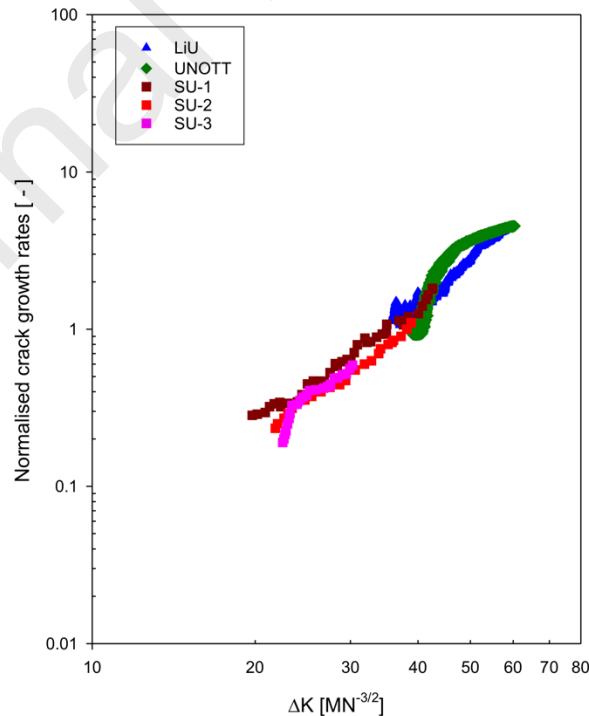

10

Figure 5: Comparison between TMF OP round robin crack growth rates measured at Linköping University (LiU), Swansea University (SU) and the University of Nottingham (UNOTT)

3.2 IP TMF crack growth round robin results

Comparison of the TMF crack growth rates under IP conditions is presented in Figure 6. Although the specimen type was different between laboratories, no difference between the test data was observed in Figure 6 except for two tests, i.e. LiU-1 and LiU-3. It can be seen that LiU-1 gave the fastest crack growth rate while the slowest IP TMF crack growth rate was measured in LiU-3. There could be several reasons to this discrepancy, e.g. microstructure, pre-cracking, crack closure effect, etc.

It is well known that microstructural factors such as grain size, size and distribution of participates have an effect on crack growth rates, especially in time dependent fatigue regime at higher temperatures, see for example [5] [14] [15] [16] [17] [18]. It is generally accepted that grain coarsening gives decrease in fatigue crack growth rates due to reduced number of grain boundaries and crack deflection [16]. Further, crack growth rates have been correlated to size and volume fraction of γ' precipitates with a decrease in crack growth rates for microstructure with larger secondary and tertiary γ' and higher volume fraction of primary γ' due to stress relaxation at the crack tip [5] [16]. The tertiary γ' size in the grains, rather than secondary γ' size, had the largest influence on the stress relaxation and therefore fatigue crack growth resistance [18]. It was also found that γ' precipitates did not have influence on fatigue crack growth at lower temperature of 427 ^{o}C.

Analysis of grain size and its distribution in all LiU IP samples with electron beams scatter diffraction (EBSD) did not reveal any inhomogeneity between the samples. Further work has been focused on characterisation of secondary and tertiary γ' precipitates in LiU-1, LiU-2 and LiU-3. As crack growth rates between LiU-2 and LiU-4 overlap at higher ΔK (> 40), initial focus has been on to compare differences in microstructure between LiU-2 and LiU-1. So far, it has been observed that there is a difference in the size and shape of both secondary and tertiary γ' precipitates between the LiU-1 and LiU-2 samples. It appears that the test specimen with the fastest crack growth rate (i.e. LiU-1) has a higher volume fraction of secondary and tertiary γ' precipitates that are smaller and rounder in shape. Currently, a work at the universities is focused on characterisation of tertiary γ' precipitates, their size and distribution variations in all the IP specimens. The main hypothesis is that tertiary γ' size and volume fraction are responsible for difference in the TMF IP crack growth rates, namely smaller size and lesser amount of tertiary γ' precipitates are associated with higher crack growth rates [19].
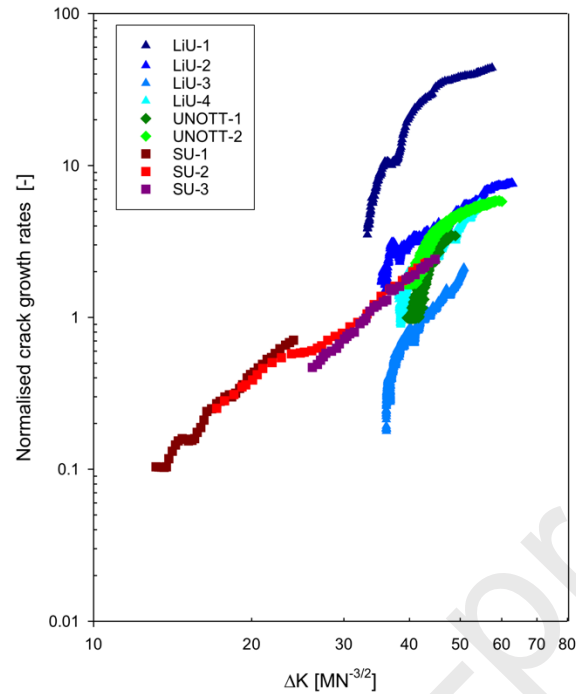
11

Figure 6: Comparison between TMF IP round robin crack growth rates measured at Linköping University (LiU), Swansea University (SU) and the University of Nottingham (UNOTT)

Crack growth rates can be affected by compressive stress states at pre-cracking due to load history effects that influence subsequent fatigue crack growth test data [20]. Compressive yielding can occur at the notch resulting in a local tensile residual stress at the crack tip, which contributes to the local driving force promoting higher crack growth rates [21] . However, it has also been found that there is no difference in crack growth rates between the traditional and compression pre-cracking after the crack propagates through three times size of the notch tip plastic zone [21]. In addition, crack closure can also affect the crack driving force caused by residual plastic deformations remaining in the wake of an advancing crack tip.

In order to understand effect of local stresses and crack closure on the crack growth rates, the behaviour of the crack tip was analysed at Linköping University using digital image correlation (DIC) images taken of the side of the SEN specimen at a frequency of 1Hz, [22]. For all DIC analyses, the reference image, and hence the state defined as zero strain state, was always taken as the image captured at zero applied stress of the same cycle as the correlated image, i.e. the instant when the temperature was 400 °C. The CTOD was obtained by looking at the vertical displacement component at a distance of 10 μm behind the crack tip and by assessing the discontinuous jump in the displacement component when going from the lower to the upper crack face. The displacement fields were smoothed and then differentiated in order to obtain the strain field from where the mechanical strain was calculated by subtracting the thermal strain from the TMF pre-test procedure. Based on the CTOD measurement, crack closure was defined as the applied stress when CTOD exceeds 1 μm. To increase the reliability of this measurement, the average stress-CTOD curve over three subsequent cycles was considered, which roughly corresponded to the minimum detectable opening in view of the scatter over these three cycles. The crack-opening stress was assessed at crack length of 3 mm in all tests, which were used as a representative value for the whole tests. It has been found that the pre-

12

cracking procedure does not affect the effective crack propagation rate calculated by compensating for the crack opening stress measured by the DIC but the amount of crack closure [22]. However, further work looking at time dependent damage accumulation, stress field at the crack tip and plasticity when the use of ΔK becomes questionable is on-going at Linköping University and the University of Nottingham.

Results from the project internal TMF CG round robin exercise described above are being translated into an internal local CoP that will be produced at the end of the project and shared with the community through the High Temperature Mechanical Testing Committee (HTMTC) for further dissemination. DevTMF has been the first advance towards validation procedures of TMF CG experimental method to be included in the CoP. However, further methodological development with a more systematic and comprehensive approach (e.g. strain control, other specimen designs, different materials, etc.) are required to identify possible variations in TMF CG response for standardisation of TMF CG method.

4. Conclusions

The work described in the present paper gives a condensed evaluation of factors that can affect accuracy and comparability of stress-controlled TMF CG testing results with an aim to produce an internal CoP between the three participating laboratories. For this reason, project internal TMF CG round robin tests on coarse grain nickel-base alloy RR1000 were carried out using corner crack and single edge notched specimens. The effect of specimen type, pre-cracking procedure, crack growth measurement approach, temperature measurements and heating methods was investigated. The results are summarised as follows:

1. The two specimen geometries used, namely corner crack and single edge notched, resulted in similar TMF CG rates.
2. Consistent and comparable TMF CG rates under OP conditions were measured.
3. TMF CG rates under IP conditions can be sensitive to the size and distribution of secondary and tertiary γ´ precipitates as observed in LiU-1 and LiU-2. Further work is on-going to characterise microstructure of the remain IP specimens.
4. Pre-cracking procedures may affect TMF CG rates, i.e. the pre-cracking of LiU-1 was performed with the TMF IP test conditions, which could have resulted in higher TMF CG rates from tensile loading at the crack tip. However, the crack growth variations observed in the LiU IP tests cancelled when compensating for crack closure, [22]. Further investigations are on-going to evaluate influence of stresses and stress gradients at the crack tip.
5. Studies of effect of induction coils with various coil setups and radiant heating on TMF CG rates as well as crack tip heating did not find any undesired heating at the crack tip. Anyway, the two types of heating methods studied have negligible impact on the TMF CG rates.
6. Three temperature measurement methods were assessed. Pyrometry and thermography offer non-invasive measurements, however, they require no change in surface emissivity during testing. Thermocouples are unfavourable to weld and are complex to set up. Rigorous control of thermocouple shielding and attachment is required in order to get accurate temperature measurements.
7. The techniques used for crack growth measurements produce results in good agreement regarding the TMF CG data. In the fourteen specimens that were tested in total, the difference

13

in the CG rates was only observed in two specimens, which can be attributed to microstructural differences, crack closure, etc.

8. An internal CoP will be produced at the end of the project. It will provide guidelines for specimen design, pre-cracking, temperature and crack growth measurements, heating methods, testing and data analysis. It should be noted that, for future validations, it will be useful to statistically plan round robin tests with a sufficient number of participants with agreed experimental protocol, apparatus, specimen type, etc.

5. Acknowledgement

6. References

[1] The Community Research and Development Information Service (CORDIS). EU research results. Thermo-mechanical fatigue - the route to standardisation (TMF-STANDARD), grant agreement ID: G6RD-CT-2001-00526; 2005.

[2] Hähner P, Rinaldi C, Bicego V, Affeldt E, Brendel T, Andersson H, Beck T, Klingelhöffer, H, Kühn H-J, Köster A, Loveday M, Marchionni M, Rae C. Research and development into a European code-of-practice for strain-controlled thermo-mechanical fatigue testing. Int J Fatigue 2008;30(2):372-381. https://doi.org/10.1016/j.ijfatigue.2007.01.052.

[3] ASTM E2368-10, Standard Practice for Strain Controlled Thermomechanical Fatigue Testing, ASTM International, West Conshohocken, PA, DOI: 10.1520/E2368-10R17; 2017.

[4] ISO 12111:2011, Metallic materials - Fatigue testing - Strain-controlled thermomechanical fatigue testing method; 2017.

[5] Li HY, Sun JF, Hardy MC, Evans HE, Williams SJ, Doel TJA and Bowen P. Effects of microstructure on high temperature dwell fatigue crack growth in a coarse grain PM nickel-based superalloy. Acta Mater 2015;90:355–369. http://dx.doi.org/10.1016/j.actamat.2015.02.023

[6] Collins, DM, Heenan RK and Stone HJ. Characterization of Gamma Prime (γ′) Precipitates in a Polycrystalline Nickel-Base Superalloy Using Small-Angle Neutron Scattering. Metall and Mat Trans A 2011;42(1):49-59. https://doi.org/10.1007/s11661-010-0466-1.

[7] Mitchell RJ, Hardy M, Preuss M and Tin S. Development of γ' Morphology in P/M Rotor Disc Alloys During Heat Treatment. Proceedings of the Tenth International Symposium on Superalloys held September 19 - 23, 2004, at the Seven Springs Mountain Resort in Champion, Pennsylvania. The Minerals, Metals & Materials Society. DOI: 10.7449/2004/Superalloys_2004_361_370.

[8] Palmer J, Jones J, Dyer A, Smith R, Lancaster R and Whittaker M. Development of test facilities for thermo-mechanical fatigue testing. Int J Fatigue 2019;121:208-218. https://doi.org/10.1016/j.ijfatigue.2018.12.015.

[9] Jones J. Enhancing the Accuracy of Advanced High Temperature Mechanical Testing through Thermography. Applied Sciences 2018;8(3):380. DOI: 10.3390/app8030380.

[10] ASTM E647-15e1, Standard Test Method for Measurement of Fatigue Crack Growth Rates, ASTM International, West Conshohocken, PA; 2015.

[11] Ewest D, Almroth P, Sjödin B, Simonsson K, Leidermark D and Moverare J. A modified compliance method for fatigue crack propagation applied on a single edge notch specimen. Int J Fatigue 2016;92(1):61-70. https://doi.org/10.1016/j.ijfatigue.2016.06.023.

[12] Norman V, Skoglund P, Leidermark D and Moverare J. The transition from micro- to macrocrack growth in compacted graphite iron subjected to thermo-mechanical fatigue. Eng Fract Mech 2017;186:268-282. https://doi.org/10.1016/j.engfracmech.2017.10.017.

[13] Pickard AC. The application of 3-dimensional finite element methods to fracture mechanics and fatigue life prediction. Warley, England: Engineering Materials Advisory Services; 1986.

[14] Bain KR, Gambone ML, Hyzak JM and Thomas MC. Development of damage tolerant microstructures in Udimet 720. Proceedings of the Sixth International Symposium on Superalloys. TMS; 1988:13-22.

[15] Hide NJ, Henderson MB and Reed PAS. Effects of grain and precipitate size variation on creep-fatigue behaviour of Udimet 720Li in both air and vacuum. In Superalloys 2000: From the 9th International Symposium on Superalloys 2000, Champion, Pennsylvania, September 17-21 2000. Minerals, Metals and Materials Society; 2000:495-503.

[16] Pang HT and Reed PAS. Fatigue crack initiation and short crack growth in nickel-base turbine disc alloys—the effects of microstructure and operating parameters. Int J Fatigue 2003;25(9-11):1089-1099. https://doi.org/10.1016/S0142-1123(03)00146-4.

[17] Pédron JP and Pineau A. The effect of microstructure and environment on the crack growth behaviour of Inconel 718 alloy at 650 °C under fatigue, creep and combined loading. Mater Sci Eng 1982;56(2):143-156. https://doi.org/10.1016/0025-5416(82)90167-7.

[18] Telesman J, Gabb TP and Gayda J. Effect of Microstructure on Time Dependent Fatigue Crack Growth Behavior In a P/M Turbine Disk Alloy. From the 11th International Symposium on Superalloys 2008, Champion, Pennsylvania, September 14-18 2008. DOI:10.7449/2008/Superalloys_2008_807_816.

[19] Engel B, Rouse JP, Lavie W, Leidermark D, Stekovic S, Hyde CJ, Williams SJ, Pattison SJ, Grant B, Whittaker MT, Jones JP. The prediction of crack propagation in coarse grain RR1000 using a unified modelling approach. Submitted to Int J Fatigue for review.

[20] Borz M, Chadwick M, Branin A and Riddell W. Fatigue Crack Growth from Compression Pre-Cracks. *Mater Perform Character* 4 2015;2(143-156). https://doi.org/10.1520/MPC20140031

[21] James M, Forth S and Newman J. Load History Effects Resulting from Compression Precracking. Journal of ASTM International 2 2005;2(9):1-17. https://doi.org/10.1520/JAI12025.

[22] Norman V, Stekovic S, Jones J, Whittaker M and Grant B. On the mechanistic difference between in-phase and out-of-phase thermo-mechanical fatigue crack growth. Int J Fatigue 2020;135:105528. https://doi.org/10.1016/j.ijfatigue.2020.105528.

15

Declaration of interests

☒ The authors declare that they have no known competing financial interests or personal relationships that could have appeared to influence the work reported in this paper.

☐The authors declare the following financial interests/personal relationships which may be considered as potential competing interests: